Rensselaer Polytechnic Institute

Troy, New York

GRANT no. NsG 48-60

NATIONAL AERONAUTICS AND
SPACE ADMINISTRATION

SEMIANNUAL STATUS REPORT NO. 8

May 1 - October 31, 1963

Submitted by

E. H. Holt

Professor of Electrical Engineering

November 1963

TABLE OF CONTENTS

SUMMARY

11532

The conventional treatment of electromagnetic wave propagation through magnetoplasmas has been critically examined. The assumption that free electrons oscillate at the same frequency as the disturbing wave is, in general, not valid for a cold, collisionless plasma. However, the theory of signal wave propagation is unaltered as the identical dispersion relation is obtained. The rigorous solution for the particle trajectories has been shown to imply the existence of a mode of propagation at the cyclotron frequency driven by the wave at the signal frequency. This type of wave has been named the "H" (for hybrid) mode. A general dispersion relation for H waves has been derived. A study of the early afterglow in nitrogen by a reflection type of microwave measurement has been made. The electron beam-plasma interaction study has been concluded with an analysis of the harmonic content of the linear accelerator beam. This confirms that there is substantial power in the sixteenth harmonic at 20.8 kmc. The conclusion of the experiment is that the plasma phenomena stimulated in previous experiments of this type were insignificant in our experiment and that the anticipated mechanism of energy leakage from the plasma is a very weak coupling effect.

AUTHOR

Publications, Technical Reports and Theses

A. Publications

1. W. C. Taft, K. C. Stotz and E. H. Holt, "A Gated Radiometer for Plasma Afterglow Study". Trans. IEEE, Instrumentation and Measurement. 12 (1963), also IEEE International Convention Record, Part 3, p.172 (1963).

2. J. E. Rudzki and E. H. Holt, "Ten Kilogauss, Air Cooled Magnet for Plasma Research", Rev. Sci. Instr. 34, 1155 (1963).

3. E. H. Holt and K. C. Stotz, "Plasma Waveguide Cell for Afterglow Measurements", Rev. Sci. Instr. 34, 1285 (1963).

4. K. C. Stotz, "Investigation of Plasma Afterglows with Application in Nitrogen", NASA Technical Note D-2226, Nov. 1963.

B. Technical Reports

1. K. C. Stotz, See item 4 above, also Plasma Research Laboratory, Tech. Rep. No. 9, June 1963.

2. R. E. Haskell, "Polarization Transforming Properties of Anisotropic Plasmas", Plasma Research Laboratory, Tech. Rep. No. 8, August 1963.

3. D. A. Huchital, "On the Existence of Cyclotron Frequency Waves in a Cold, Collisionless, Anisotropic Plasma". Plasma Research Laboratory, Tech. Rep. No. 10, August 1963.

4. E. H. Holt, "The Plasma Research Laboratory. A Status Report". Plasma Research Laboratory, July 1963.

C. Theses

1. J. S. Mendell, "Investigation of Plasma Oscillations Stimulated by a Pre-Bunched Electron Beam from the RPI Accelerator". Rensselaer Polytechnic Institute, Ph.D. Thesis, September 1963.

2. K. C. Stotz, See item 4, Section A, above. Rensselaer Polytechnic Institute, Ph.D Thesis, June 1963.

3. R. E. Haskell, "Polarization Transformations with Applications to Anisotropic Plasmas". Rensselaer Polytechnic Institute, Ph.D. Thesis, June 1963.

4. D. A. Huchital, See item 3, Section B, above. Rensselaer Polytechnic Institute, M.E.E. Thesis, August 1963.

5. W. C. Schwartz, "A Microwave Reflection Method for the Investigation of Uniform Dense Plasmas". Rensselaer Polytechnic Institute, M.E.E. Thesis, August 1963.

6. J. J. Sirota, "Design of a Time-of-Flight Mass Spectrometer", Rensselaer Polytechnic Institute, B.E.E. Thesis, June 1963.

7. R. A. Bitzer, "A Microwave Lens System for use in the Plasma Laboratory". Rensselaer Polytechnic Institute, M.E.E. Thesis, January 1963. (not listed in the previous status report)

1. Electromagnetic Wave Propagation in Magnetoplasmas.

1.1 Introduction

A critical theoretical and experimental analysis of the conventional theory of electromagnetic wave propagation in magnetoplasmas is being pursued. Mathematically, we are required to solve for the currents caused by the wave simultaneously with Maxwell's equations. A first step is thus the solution of the equation of motion for the electrons,

$$m\dot{v}_i = -eE_i - e\epsilon_{ijk} v_j B_k^{\circ} \qquad (1)$$

where E_i is the electric field of the wave and B_k° is the magnetic field in which the plasma is immersed.

Now it is conventional to argue that the velocity of the electrons, v_i, has the same time dependence as the electric field of the wave. For example, if we refer back to the earliest discussions, we encounter,

> E. V. Appleton, in the Journal of the Institution of Electrical Engineers, 1932,
>
> " . . . let us assume that all the field vectors are represented by expressions containing the factor $e^{i(pt-qx)}$."

and

> D. R. Hartree, in The Proceedings of the Cambridge Philosophical Society, 1931,
>
> " . . . then, taking the forced oscillations only, . . ."
>
> (There follows a set of equations in which the time dependence of all quantities is taken as $e^{i\omega t}$)

and, if we study a more recent discussion, we discover,

T. H. Stix, in The Theory of Plasma Waves, 1962,

" . . . and since there is no zero order thermal motion, $\frac{d\bar{v}_k}{dt} = -i\omega\bar{v}_k$."

However, in this case, where the magnetic field is static and uniform, the equation of motion is readily solved, so that this assumption is unnecessary. Furthermore, it will be seen that the assumption submerges an important portion of the solution.

This situation has motivated a theoretical and experimental effort in this laboratory.

1.2 Theory of Electronic Orbits in Magnetoplasmas

A. Conventional Theory.

It is required to solve

$$m\dot{v}_i = -eE_i - e\epsilon_{ijk} v_j B_k^{\circ} \tag{1}$$

where

E_i is the electric field of the wave, varying as $e^{i\omega t}$

B_k is the magnetic field in which the plasma is immersed.

Now the critical assumption takes the form

$$\dot{v}_i = i\omega v_i \tag{2}$$

It can now be readily shown that if B is in the x_3 direction, the v_i are related to the electric field of the wave by

$$\begin{bmatrix} v_1 \\ v_2 \\ v_3 \end{bmatrix} = \frac{ie}{m\omega} \begin{bmatrix} 1 & iY & 0 \\ -iY & 1 & 0 \\ 0 & 0 & 1-Y^2 \end{bmatrix} \begin{bmatrix} E_1 \\ E_2 \\ E_3 \end{bmatrix} \tag{3}$$

where

$$Y = \frac{eB}{m\omega}$$

and we denote

$$\frac{eB}{m} = \Omega \text{ , the cyclotron frequency.}$$

From this point, the dielectric tensor is derived in the form[1]

$$K_{ij} = \begin{bmatrix} S & -iD & 0 \\ iD & S & 0 \\ 0 & 0 & P \end{bmatrix}$$

where

$$S = 1 - \frac{X}{1-Y^2} \; ; \quad D = \frac{XY}{1-Y^2} \quad ; \quad P = 1 - X$$

$$X = \frac{\omega_p{}^2}{\omega^2} = \frac{Ne^2}{m\epsilon_o\omega^2}$$

and N is the electron number density.

B. Modified Theory

The point of the current effort is, of course, that the problem can be solved without making the assumption

$$\dot{v}_i = i\omega v_i$$

The rigorous solution to equation (1) is of the form[2]

$$v_1(t) = -f_1 \frac{\omega}{\Omega^2-\omega^2} (\cos \omega t - \cos \Omega t) + f_2 \frac{\Omega}{\Omega^2-\omega^2} \sin(\omega t+\phi)$$

$$-\tilde{f}_2 \frac{\Omega}{\Omega^2-\omega^2} \cos \Omega t - \underset{\sim}{f}_2 \frac{\omega}{\Omega^2-\omega^2} \sin \Omega t \tag{5}$$

$$+ v_1^o \cos \Omega t - v_2^o \sin \Omega t$$

$$v_2(t) = -f_1 \frac{1}{\Omega^2-\omega^2} (\Omega \sin \omega t - \omega \sin \Omega t) - f_2 \frac{\omega}{\Omega^2-\omega^2} \cos(\omega t+\phi)$$

$$+ \underset{\sim}{f}_2 \frac{\omega}{\Omega^2-\omega^2} \cos \Omega t - \tilde{f}_2 \frac{\Omega}{\Omega^2-\omega^2} \sin \Omega t + v_1^o \sin \Omega t + v_2^o \cos \Omega t \tag{6}$$

$$v_3(t) = v_3^o + f_3 \cos(\omega t+\phi) \tag{7}$$

where

$$E_1 = E_1^o \sin \omega t$$

$$E_2 = E_2 \sin(\omega t+\phi) = \underset{\sim}{E}_2 \sin \omega t + \tilde{E}_2 \cos \omega t$$

$$E_3 = E_3^o \sin(\omega t+\phi) = \underset{\sim}{E}_3 \sin \omega t + \tilde{E}_3 \cos \omega t$$

$$f_i^{(o)} = \frac{e}{m} E_i^{(o)}$$

Now since we desire the orbit of an average particle in an ensemble, we examine equations (5), (6), and (7) carefully. The only terms which vary from electron to electron are those involving the initial conditions, v_i^o. Therefore, these are the only terms we must consider in taking an average. This point cannot be overemphasized, since for an isotropic distribution of initial velocities the initial condition terms average to zero and we are left with the components below.

$$\langle v_1(t) \rangle = f_1 \frac{\omega}{\Omega^2-\omega^2} (\cos \omega t - \cos \Omega t) + f_2 \frac{\Omega}{\Omega^2-\omega^2} \sin(\omega t+\phi)$$

$$- \tilde{f}_2 \frac{\Omega}{\Omega^2-\omega^2} \cos \Omega t - \underset{\sim}{f}_2 \frac{\omega}{\Omega^2-\omega^2} \sin \Omega t \tag{8}$$

$$\langle v_2(t) \rangle = -f_1 \frac{1}{\Omega^2-\omega^2} (\Omega \sin \omega t - \omega \sin \Omega t) - f_2 \frac{\omega}{\Omega^2-\omega^2} \cos(\omega t+\phi)$$

$$+ \underset{\sim}{f}_2 \frac{\omega}{\Omega^2-\omega^2} \cos \Omega t - \tilde{f}_2 \frac{\Omega}{\Omega^2-\omega^2} \sin \Omega t \tag{9}$$

$$\langle v_3(t) \rangle = f_3 \cos(\omega t+\phi) \tag{10}$$

The results expressed by equations (8), (9) and (10) are extremely important to this discussion. They indicate that the velocity of an average particle contains components at the cyclotron frequency that arise only because of the presence of the electric field of the wave, and are no less coherent than the components at the signal frequency. To be sure, there is also random motion at the cyclotron frequency, but it is a function of the initial conditions, which we have already removed.

The final trajectories are apparently strongly dependent upon the ratio Ω/ω , but it is not difficult to decide what general form the orbits take. If we separate the signal and cyclotron frequency components, we have

$$x_1(t) = -\frac{f_2}{\Omega^2-\omega^2}\,\frac{\Omega}{\omega}\cos\omega t \qquad x_1(t) = \frac{f_2}{\Omega^2-\omega^2}\,\frac{\omega}{\Omega}\cos\Omega t$$

$$x_2(t) = -\frac{f_2}{\Omega^2-\omega^2}\sin\omega t \qquad x_2(t) = \frac{f_2}{\Omega^2-\omega^2}\,\frac{\omega}{\Omega}\sin\Omega t$$

Now for the signal frequency components alone

$$\left(\frac{x_1}{\frac{f_2}{\Omega^2-\omega^2}\,\frac{\Omega}{\omega}}\right)^2 + \left(\frac{x_2}{f_2/\Omega^2-\omega^2}\right)^2 = 1$$

This is the equation of an ellipse with semiaxes $\dfrac{f_2\,\Omega}{\omega(\Omega^2-\omega^2)}$ and $\dfrac{f_2}{\Omega^2-\omega^2}$ The ellipse is thus oriented along the x_1 axis for $\Omega/\omega > 1$ and along the x_2 axis for $\frac{\Omega}{\omega} < 1$. We note that the electron moves in the right handed sense.

The equation for the cyclotron frequency components is

$$x_1^2 + x_2^2 = \left(\frac{f_2\,\omega}{\Omega(\Omega^2-\omega^2)}\right)^2$$

which represents a circle with radius $\dfrac{f_2 \omega}{\Omega(\Omega^2-\omega^2)}$. The motion is right handed.

The significant point in this discussion is that in a plasma excited by a signal wave, the electronic motion which remains after averaging contains components both at the signal frequency and the cyclotron frequency. This result should be compared with the conventional theory which allows only for signal frequency motion. We must now consider the significance of the difference.

As a preliminary step, let us examine the conventional theory on a microscopic level. In a collisionless isotropic plasma, we picture the process as follows: as the wave propagates through the plasma, it excites electron currents, (or, alternatively, electric dipoles) in the same direction as its electric field and at the same frequency. This current, alternating as it does, radiates a <u>sub-wave</u> in the same direction and at the same frequency. It can be shown that the velocities of the electrons differ by ninety degrees from the signal wave, and that the sub-wave is in phase with the electron orbits. The final result is therefore a phase shift and amplitude modulation of the signal wave.

The problem is only moderately more complicated in an anisotropic plasma. The difference lies in the fact that the electron orbits need not be in the same direction as the electric field of the signal wave. Therefore, the sub-wave electric field is probably in a different direction from the direction of the field that caused it originally. This effect results in the well known phenomenon of Faraday rotation. The essence is that, for example, a linearly polarized wave will, besides incurring a phase shift in passing through the plasma, also generate another wave, perpendicular to it and at some phase angle from it.

Although this is a somewhat simplified picture, it is a valid approach to the problem. In fact, the entire theory of plasma waves can be derived from a microscopic theory such as this as opposed to the favored macroscopic approach.

This, however, is the conventional theory. The preceding analysis has indicated the following addition: that besides being responsible for all the previously mentioned phenomena, the electrons also oscillate coherently at the cyclotron frequency. In terms of the previous argument, we infer the radiation of a second sub-wave at the cyclotron frequency which may differ considerably in phase and polarization from the signal wave. This wave then propagates according to the previous arguments, obediently generating its own set of sub-waves.

1.3 Characteristics of Hybrid Wave Propagation

We therefore suspect that there may exist a radiation at the cyclotron frequency from a plasma excited by a signal wave. To determine its characteristics requires the rigorous solution of the collisionless equation of motion for the electrons together with Maxwell's equations

$$\epsilon_{ijk} E_{k,j} = -\mu_0 \dot{H}_i$$
$$\epsilon_{ijk} H_{k,j} = \dot{D}_i - Nev_i$$

The results already obtained for the electron velocity, v_i , lead us to seek solutions of the form

$$E_i = E_i^{\circ} e^{i\omega t} + E_i^{*} e^{i\Omega t}$$
$$H_i = H_i^{\circ} e^{i\omega t} + H_i^{*} e^{i\Omega t}$$

with the implicit requirements that the field vectors are not functions of time. The dispersion relation for the Hybrid (or "H") wave can then be shown to be[3]

$$n_*^4 \sin^2\theta + n_*^2\left(4T-2-\sin^2\theta\right) + 4T^2 - 6T + 2 = 0$$

where

n_* is the refractive index of the plasma for the H wave.

θ is the angle between the direction of propagation and the magnetic field.

$$T = \frac{X}{2Y^2}$$

It is interesting to note that this approach to the problem in no way challenges the current theory of signal wave propagation in magnetoplasmas. The dispersion relation obtained for the wave of frequency ω is identical with the result obtained conventionally.

A possibly significant aspect of the phenomenon becomes apparent when the energy balance between the H and signal waves is examined. If we denote the ratio of H-wave power to signal frequency power as μ, we find that[4]

$$\mu = \left\{\frac{X}{(n_*^2-1)\,Y\,(Y\pm 1)}\right\}^2$$

where the positive sign is taken if the signal wave is left hand circularly polarized in the x_1-x_2 plane, and the negative sign applies if the wave is right hand polarized in the same plane.

The interesting point in this discussion is that for this right hand circularly polarized component of the signal wave, μ exhibits a pole at $Y = 1$. Thus the H wave principle would appear to indicate a possibly significant deterioration of the propagating characteristics of a magnetoplasma in the vicinity of cyclotron resonance.

1.4 Experimental Analysis

An experiment is presently being prepared to study this theory. The objectives are

1. To observe and study the characteristics of H wave propagation.

2. To determine the effects of electron-neutral collisions.

3. To study the transmission properties of a magnetoplasma in the vicinity of cyclotron resonance.

The experiment will be performed in a guided wave configuration at X-band frequencies. The plasma diagnosis and transmission measurements will be accomplished by the polarization techniques developed in this laboratory by Dr. R. E. Haskell.[5] The experiment can be performed with an available magnetic field ranging in strength from several hundred to ten thousand gauss.[6]

2. Basic Plasma Processes

2.1 Afterglow Studies in Nitrogen; Summary

Following initial measurements of electron loss coefficients in the nitrogen afterglow (reported in the previous progress report), several questions remained unanswered. During the past six months, attempts to answer some of these questions were made, and the experiments were extended to include measurements of electron collision cross-sections.

During the initial measurements mentioned above, the electron temperature was found to increase after the removal of the source of ionization. The increase in electron temperature was attributed to the presence of metastable molecules, which through metastable-metastable collisions would produce hot electrons. In order to investigate the dense early afterglow, a method of measurement based on the complex reflection coefficient of a plasma-air boundary was developed and is discussed below.

The availability of the gated microwave radiometer to measure electron energy has led to an attempt to measure the electron collision cross-section as a function of energy in the afterglow. The collision cross-section is obtained from attenuation and phase shift measurements of a microwave signal passing through the plasma while the energy is being measured by the gated microwave radiometer. Some improvements to the radiometer are mentioned in a later section.

2.2 Reflection Measurements

In the early afterglow where the electron density is high, a microwave signal transmitted through the plasma is severely attenuated so that little information is obtained. In order to overcome this difficulty, the reflected signal from the plasma was monitored. The spatial electron density distribution was assumed uniform since recombination is the predominant loss mechanism in the early afterglow and plane boundaries are assumed. The configuration then becomes the one indicated in figure 1. The total complex reflection coefficient from this configuration is

$$\rho_T = \rho \left[\frac{1 - \epsilon^{-2\gamma_2 L}}{1 - \rho^2 \epsilon^{-2\gamma_2 L}} \right]$$

where ρ is the complex reflection coefficient for the first plane boundary and γ_2 is the complex propagation constant of the plasma-filled portion of waveguide. The conductivity of the plasma was taken from the model of a weakly ionized gas to be

$$\sigma_p = \frac{N_e q^2}{m} \left(\frac{\nu - j\omega}{\nu^2 + \omega^2} \right)$$

where ν is the effective collision frequency for momentum transfer. Measurement of the complex reflection coefficient determines σ_p, thus the electron density and collision frequency are obtained. Results of measurements of electron density by this method in nitrogen are shown in figure 2.

The electron density does not show a perceptible rise. The energy imparted to the plasma during each breakdown pulse was approximately 10 millijoules. With increased energy plasmas, the metastable population might increase to the point where metastable-metastable collisions would increase the electron density in the early afterglow. A technical difficulty encountered here is that the hollow cathode waveguide plasma cell requires a positive breakdown pulse (so that the entire waveguide circuit remains at ground potential). The present method of pulse generation is to invert the negative

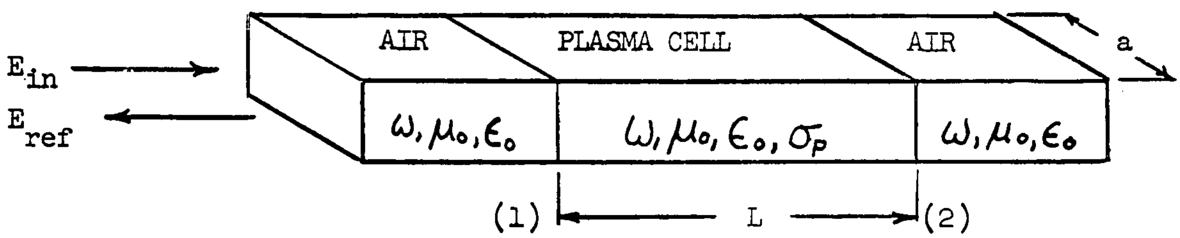

Figure 1

Propagation of Electromagnetic Waves in a Plasma Cell.

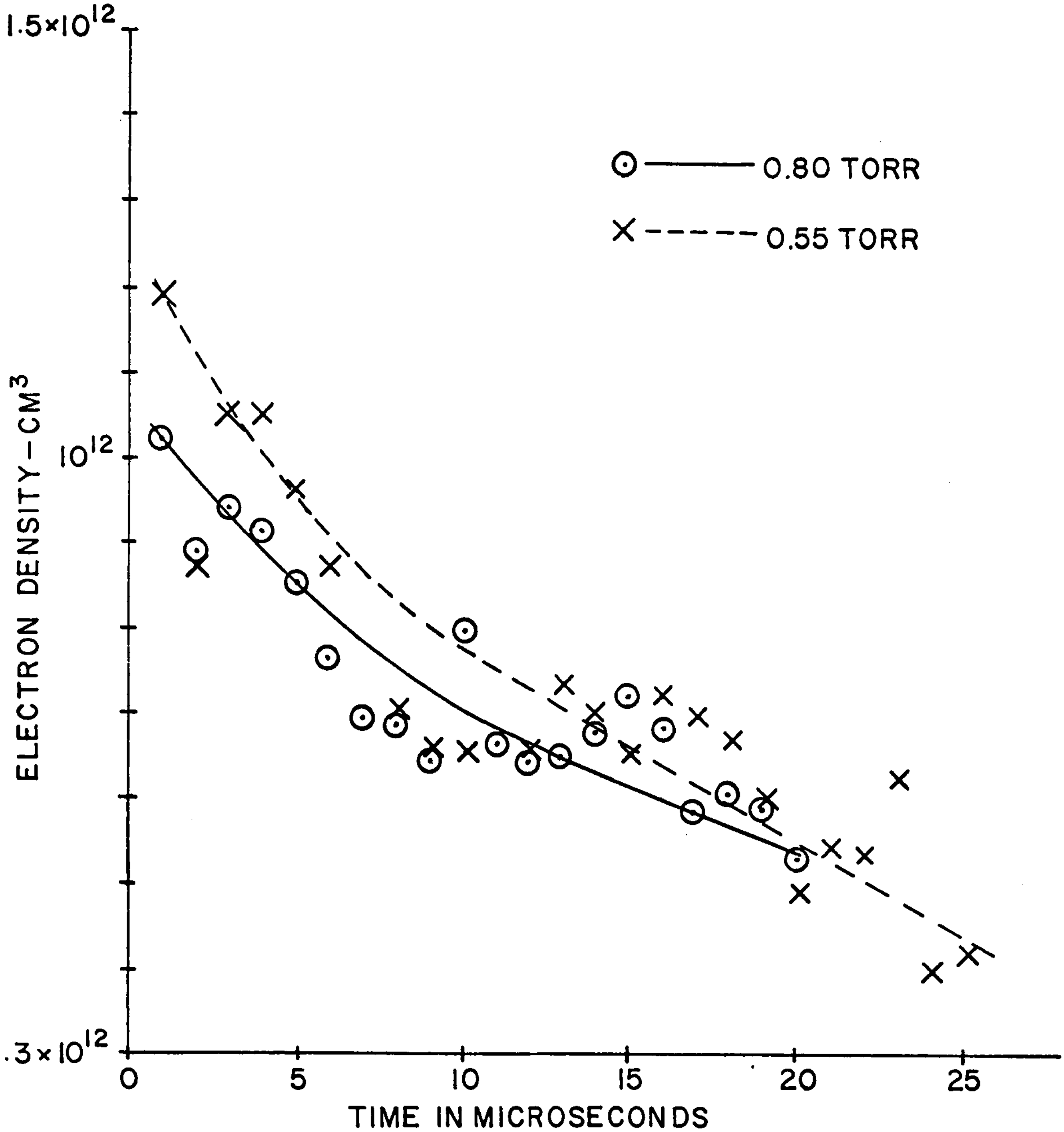

Figure 2

Electron Density in the Early Afterglow of Nitrogen.

output of a hard tube pulser with a pulse transformer. Since practical limitations are placed on the product of current-time passed through the pulse transformer a positive pulse generator with improved current capability is being developed.

2.3 Gated Microwave Radiometer

The gated microwave radiometer has been successful in the measurement of electron temperature variations in the afterglow. Some modifications to the original model have been made to increase the usefulness of the device. A new I.F. amplifier with a 20 megacycle bandwidth has been designed with a resultant gain in sensitivity of a factor of $\sqrt{2}$. The phase detector and DC amplifier chassis have been redesigned for increased stability, and a decrease in output drift has been obtained. The timing circuits in the original model consisted of various commercial pulse generators and delay networks. All timing elements have now been redesigned and constructed in one transistorized chassis.

2.4 Mass Spectrometer

After a break during the summer months the time-of-flight mass spectrometer project has been reactivated.

3. Electron Beam-Plasma Interaction.

3.1 Summary

Following the sub-threshold result reported in the previous status report an analysis has been made of the harmonic content of the Linac beam. This analysis confirms the previous assumption that there is substantial power in the sixteenth harmonic at 20.8 kmc.

Theoretical considerations have also been derived from a different point of view.

Both of these developments will be reported briefly here. A fuller report will be prepared separately. The conclusion of the experiment is that the plasma phenomena stimulated in previous experiments of this type were insignificant in our experiment and that the anticipated mechanism of energy leakage from the plasma is a very weak coupling effect.

3.2 The Calculation of the 16th Harmonic of the Linac Beam

3.2.1 Harmonic Analysis of the Linac Beam

The periodic nature of the density of the electron bunches from the Linac beam enables an analysis in terms of Fourier components to be conveniently made.

Thus:

$$\rho\,(z-ut) = \frac{q}{\pi a^2 u T} \sum_{N=-\infty}^{\infty} \eta_N \exp\left[i\, \frac{\omega_N}{u} (z-ut) \right] \quad \text{--- } 1$$

where, Linac operating frequency $\omega_L = 2\pi \times 1.3 \times 10^9$ per sec.

Linac electron speed $u = 3 \times 10^8$ m/sec.

the beam moves in the z direction.

The beam charge density ρ is therefore a function of $z - ut$

q is the total charge in a bunch.

The harmonic frequencies $\omega_N = N\,\omega_L$

The cross-sectional area of a bunch is πa^2

The periodic time between bunches, $T = 2\pi/\omega_L$

The factor $\frac{q}{\pi a^2 uT}$ is, therefore, the average charge density per cycle.

It can be shown that

$$\eta_N = C_N / 2C_0$$

where,

$$C_N = \int_0^T \rho(t) \exp[i\omega_N t]\, dt$$

and,

$$C_0 = \frac{1}{2}\int_0^T \rho(t)\, dt$$

3.2.2 The Acceleration of Electrons in the Linear Accelerator

Acceleration occurs in a series of nine identical microwave cavities, which are excited by high power klystrons. If the phase relationship between cavities is properly adjusted, a wave will propagate down the accelerator with the speed of light. This wave is known as the synchronous wave because electrons traveling down the accelerator with speeds close to 3×10^{10} cm/sec maintain an almost constant phase relationship with the wave.

The electrons are injected with an energy of 100 kev. They are compressed into bunches by the klystron-like section of a buncher cavity. Then they enter the first rf cavity, in which their energy is increased to several Mev. Upon leaving the first cavity the electrons are traveling at very close to the speed of light and are almost synchronous with the accelerating wave.

The extent to which the electrons lag in phase behind the synchronous wave can be shown to be given by

$$\Delta \phi = -\frac{\omega}{c} \, 8 \cdot 2 \left(\frac{1}{W_i} - \frac{1}{W_f} \right) \qquad --- \quad 2$$

where $\Delta\phi$ is the phase difference in degrees

ω is the frequency of the wave

c is the speed of light

W_i, W_f are the initial and final electron energies when the electron travels a certain distance in the accelerator. The following table is calculated from equation 2.

Initial energy Mev	Final energy Mev	Phase lag o
3	5	1.07
5	10	0.82
10	15	0.28
15	20	0.13
20	25	0.08

Thus the phase lag above 3 Mev can be neglected.

The total energy of an electron emerging from the Linac is the sum of the energy which it acquired before achieving synchronism (3 Mev) plus the integral of force times distance in the remainder of the accelerator. The electrons which are accelerated in the machine are typically disposed in phase as shown in figure 3 and do not in consequence all acquire the same energy. In fact the foremost electrons ($\phi=\phi_1$) are the least energetic.

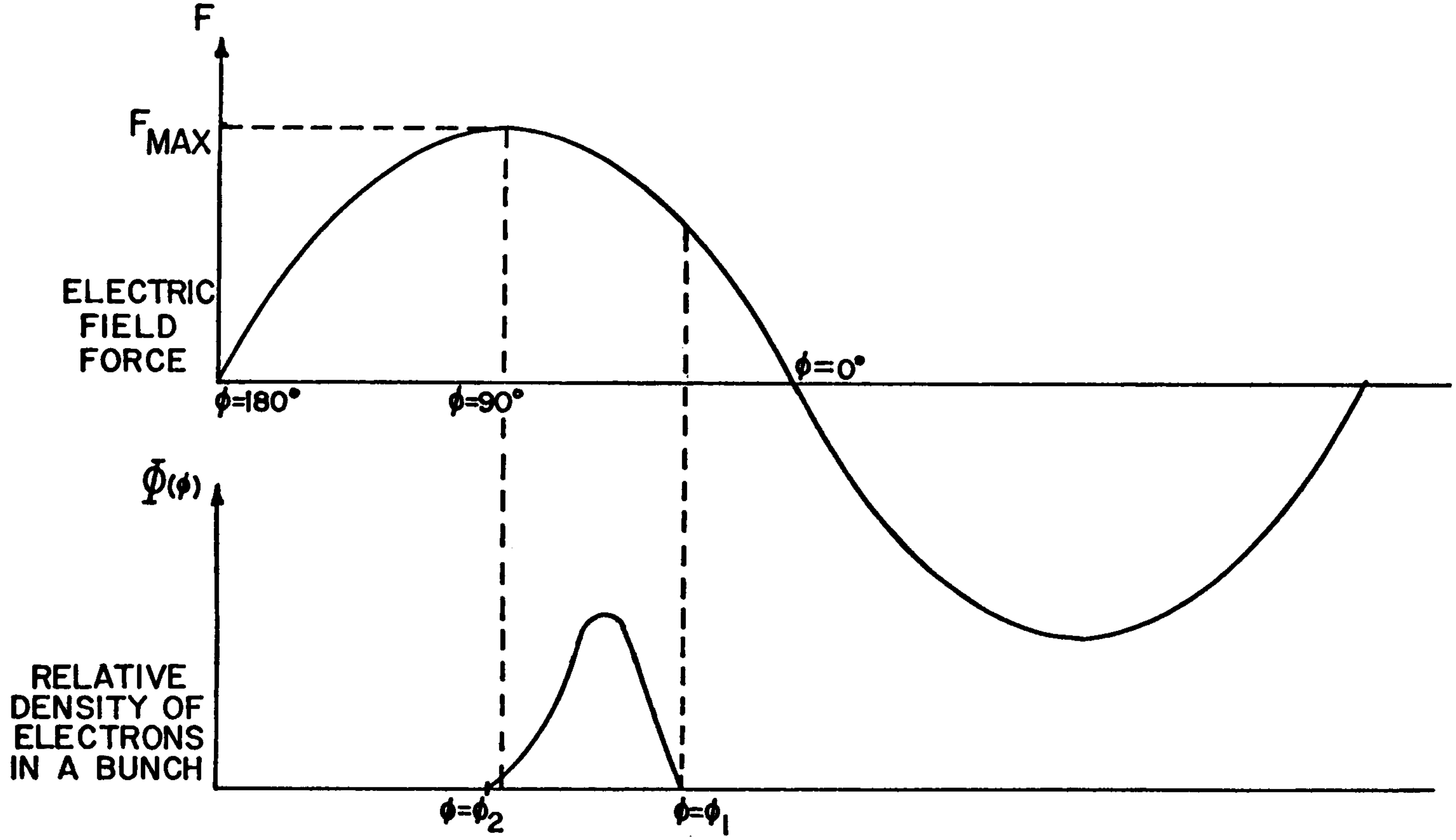

Figure 3

Phase of Electrons Accelerated by the Linac.

3.2.3 The Distribution of Electrons in a Bunch

The energy spectrum of electrons is measured with a magnetic analyser. Three steps are necessary to convert the raw data into a plot of the electron density as a function of position.

Because of the physical principal of the analysis the graph of the current collected by the Faraday cup as a function of the magnetic field strength is a distorted form of the energy spectrum. This must be corrected first.

In the second step we convert the graph to one showing the phase distribution of the electrons and thirdly we convert to a distribution of charge as a function of position. This has been done for 4 representative sets of analyser data.

For each set of data a Fourier analysis has been performed for the first 32 harmonics.

3.2.4 The Sixteenth Harmonic at 20.8 Kilomegacycles

The values of η_{16} (equation 1) for the four cases are 0.31, 0.35, 0.30 and 0.39. Thus the Linac beam can be said to have a substantial sixteenth harmonic content.

The distributions were calculated on the assumption that electrons become synchronous with the wave at 3 Mev. Slightly larger or smaller values might have been used and would have resulted in slightly different values of η_{16} .

The Linac beam charge density for the sixteenth harmonic is

$$\rho_{16} = \frac{q}{\pi a^2 u T} \eta_{16} \exp\left[i \frac{\omega_{16}}{u} (z - ut) \right]$$

This is the average density. The beam is actually densest on its axis. The density on the axis is approximately twice the average density. When the peak beam current is 0.3 A the charge per bunch is

$$\frac{0.3\ \text{A}}{1.3 \times 10^{9}/\text{sec}} = 2.3 \times 10^{10}\ \text{coulomb}$$

Also

$$\eta_{16} = 0.3$$

$$\pi a^2 = 2 \times 10^{-4}\ \text{m}^2$$

$$ut = 0.23\ \text{m}$$

so that

$$\rho_{16} = 1.5 \times 10^{-6}\ \frac{\text{coul}}{\text{m}^3} \qquad \text{--- } 2a$$

3.3 Theoretical Considerations

3.3.1 Calculation of the Power Extracted from the Beam in Steady State

We can show that the dielectric coefficient of the plasma, ε_r , can be written in the form

$$\varepsilon_r = 2\frac{\Delta\omega}{\omega_p} + i\frac{\nu}{\omega_p} \qquad \text{--- } 3$$

where $\Delta\omega = \omega - \omega_p$

ω is the frequency of the sixteenth harmonic

ω_p is the plasma frequency

ν is the electron collision frequency

Also we can show that

$$\bar{\nabla} \times \bar{H} = -i\omega \varepsilon_0 \varepsilon_r \bar{E} + \rho \bar{u} \qquad --- 4$$

where $\bar{E}$, $\bar{H}$ are the fields associated with the plasma oscillations

ρ is the charge density in the beam

$\bar{u}$ is the beam velocity

Equation 4 can be written as

$$\bar{E} = \frac{1}{-i\omega \varepsilon_0 \varepsilon_r} \bar{\nabla} \times \bar{H} + \frac{1}{i\omega \varepsilon_0 \varepsilon_r} \rho \bar{u} \qquad 5$$

The first term on the right-hand side is the contribution to the electric field due to the curl of the magnetic field set up by the beam. To solve for this term would involve setting up the boundary value problem for the electric and magnetic fields stimulated by a beam traversing a non-uniform plasma, a problem which would be very difficult. The second term, however, depends on the beam charge density and the plasma density where the beam passes through the plasma. Considering only the second term, which will be called $\bar{E}'$, equation 5 becomes

$$\bar{E}' = \frac{1}{i\omega \varepsilon_0 \varepsilon_r} \rho \bar{u} = \frac{1}{i\omega \varepsilon_0 \varepsilon_r} \bar{J} \qquad --- 6$$

When the Linac beam is turned on it sets up plasma electron oscillations. These are the superposition of two oscillations at pure frequencies; there is a damped transient oscillation at the plasma frequency and a forced oscillation at the sixteenth harmonic frequency.

Now the collision frequency is in the order of 0.3 Mc - 1.0 Mc. The transient oscillations at the plasma frequency that occur when the Linac beam is turned on will persist for several periods of collision, so that the time required for the establishment of the steady state is of the order of 3-10 μsec. Since the length of an electron burst from the Linac is only 0.1 μsec, it is not expected that the steady state will be established in this short time. Nevertheless, the steady state behavior can be calculated as a limiting example of what might occur if the beam were left on long enough.

In the steady state the average power delivered by the beam to the plasma is given by

$$P = \frac{1}{2} \text{ Real Part} \int \bar{E} \cdot \bar{j}^{*} \, dv \qquad --- \; 7$$

where the integral is taken over the interaction region, i.e., the region traversed by the beam. The length of this region is the length of the vessel, 28 cm, and the diameter of this (cylindrical) region is the diameter of the beam, 1.6 cm, for a total volume of 50 cm^3. Within this region the integrand is a function of position. Firstly, the current density of the Linac beam is a decreasing function of distance from the axis. Secondly, the plasma frequency is a decreasing function of distance from the axis, so that $\mathcal{E}_r$ is not uniform.

Substituting equation 3 in equation 6 gives

$$\bar{E}' = \frac{1}{\nu + 2i\Delta\omega} \frac{\bar{J}}{\varepsilon_0} = \frac{-\nu + 2i\Delta\omega}{\nu^2 + 4(\Delta\omega)^2} \frac{\bar{J}}{\varepsilon_0}$$

so that

$$\bar{E}' \cdot \bar{j}^* = \frac{-\nu + 2i\,\Delta\omega}{\nu^2 + 4(\Delta\omega)^2} \frac{|j|^2}{\varepsilon_0} \qquad \text{--- 8}$$

and

$$\frac{1}{2} \text{Real Part} \left[\bar{E}' \cdot \bar{j}^* \right] = -\frac{1}{2} \frac{\nu}{\nu^2 + 4(\Delta\omega)^2} \frac{|j|^2}{\varepsilon_0} \qquad \text{--- 9}$$

The integrand of equation 7 has its largest value where $\Delta\omega = 0$

$$\frac{1}{2} \text{Real Part} \left[\bar{E}' \cdot \bar{j}^* \right]_{peak} = -\frac{1}{2} \frac{1}{\nu} \frac{|j|^2}{\varepsilon_0} \qquad \text{--- 10}$$

Numerically,

$$|\dot{j}_{av}| = 1.5 \times 10^{-6} \frac{\text{coul}}{\text{m}^3} \times 3 \times 10^{8} \frac{\text{m}}{\text{sec}} = 450 \frac{\text{A}}{\text{m}^2}$$

$$\nu = 0.3 \times 10^{6}/\text{sec} \qquad \text{--- 11}$$

and

$$\frac{1}{2} \text{Real Part} \left[\bar{E}' \cdot \bar{j}^* \right] = 4 \times 10^{10} \frac{\text{watts}}{\text{m}^3} \qquad \text{--- 12}$$

An upper limit to the total power yielded by the beam can be found by multiplying this figure by the volume of the interaction region, 5×10^{-5} m^3, to give 2×10^{6} watts. Because the plasma is so non-uniform in the interaction region the maximum value of the integrand can only be attained in a very small subregion of the whole interaction region. For instance, the numerical value of the integrand may range between 4×10^4 and 4×10^{10} watts/m^3 (for $\Delta\omega/2\pi$ = 20 Mc and 0 Mc, respectively) within the interaction region, so the actual power extracted from the beam by the plasma is probably closer to 2 watts than 2 Mw.

Notice that the power figures depend upon two conditions which are not experimentally controllable, the plasma frequency and the non-uniformity of the plasma.

3.3.2 Calculation of the Energy Stored in the Electric Fields. Transient Behavior.

In the previous section it was shown that in the steady state the beam would have to furnish several kilowatts of power to maintain the plasma oscillations. This was done to show that the plasma is capable of extracting considerable power from the beam. This sort of estimate was partially responsible for our undertaking this experiment.

Since the beam actually is fired in 0.1 μsec bursts, it is perhaps better to inquire how much energy is stored in the oscillating fields during the transient response to a burst of electrons.

The energy stored in the electric fields is

$$\mathcal{E} = \int \frac{1}{2} \varepsilon_0 E^2 dv$$

Consider the transient behavior of the field during the 0.1 μsec that the beam is turned on. Unless the beam-plasma system is so close to resonance that the collisions limit the fields, it will not matter if the collision frequency is assumed equal to zero. This is a convenience that allows the transient behavior to be found by applying a simple, tabulated

Laplace transform to the steady state solution of equation 6.

To commence the Laplace transformation, write $s = i\omega$, and equation 6 becomes

$$T_{\tau}\left\{E_z'(t')\right\} = \frac{s}{s^2+\omega_p^2}\ \frac{u}{\varepsilon_0}\ T_{\tau}\left\{\rho(\tau, t')\right\} \quad \text{--- 13}$$

where

$$t' = t - z/u$$

If

$$\rho(\tau, t') = 0 \qquad t' < 0$$

$$= \rho_0(\tau)\sin\omega' t,\ t' > 0$$

Then

$$T_{\tau}\left\{\rho(\tau, t')\right\} = \rho(\tau)\frac{\omega'}{s^2+(\omega')^2} \quad \text{--- 14}$$

and

$$T_{\tau}\left\{E_z'(t')\right\} = \frac{u}{\varepsilon_0}\ \rho_0(\tau)\ \frac{s}{s^2+\omega_p^2}\ \frac{\omega'}{s^2+(\omega')^2} \quad \text{-- 15}$$

Finally,

$$E_z'(t') = 0 \qquad t' < 0$$

$$= -\frac{u}{\varepsilon_0\varepsilon_r\,\omega'}\ \frac{\rho_0(\tau)}{2}\left[\sin\frac{\omega'+\omega_p}{2}t' \,.\, \sin\frac{\Delta\omega}{2}t'\right] \quad \text{-- 16}$$

$$t' > 0$$

Besides oscillating at a frequency which is average of $\frac{\omega'}{2\pi}$ and $\frac{\omega}{2\pi}$, the electric field beats with a frequency $\frac{\Delta\omega}{2\cdot 2\pi}$. If $\frac{\Delta\omega}{2\pi}$ = 20 Mcs on the axis of the vessel, then during a 0.1 μsec burst of electrons from the Linac the electric field there will beat once. However, the fields off the axis will be beating at slightly different frequencies, depending on the local value of ω_p. Furthermore, the intensity of the fields varies with position in the vessel, since E_z' depends on ρ/ε_r. That is, since the density of the Linac beam, ρ, falls off radially, the electric field is apt to be weak near the outer edge of the beam. And because ε_r depends on ω_p, it is a function of radial position.

When the 0.1 μsec burst of Linac electrons ends, the plasma electrons continue to oscillate for a while at the plasma frequency, so that the electric field does not disappear immediately. The oscillations are eventually damped out, either because of collisions between plasma electrons and gas molecules, or because of the decay of the plasma density.

The amplitude of the electric field is

$$E_{z\,ampl}' = \frac{u}{\varepsilon_0 \varepsilon_r \omega} \frac{\rho_0(r)}{2} \qquad --- 17$$

Suppose $\frac{\omega}{2\pi}$ = 20.400 kMc and $\frac{\omega_p}{2\pi}$ = 20.380 kMc. Then $\varepsilon_r = \frac{2\Delta f}{f} = 2 \times 10^{-3}$, which means that the field in plasma is 2000 times higher than the field in free space.

For the sixteenth harmonic $\rho_0 = 1.5 \times 10^{-6}$ coulomb/m^3. Then the amplitude is

$$E_{z\,ampl}' = 8 \times 10^4 \text{ v/m}. \qquad --- 18$$

When the field strength according to equation 18, is 8 x 10^4 v/m the energy density is 0.03 joules/m^3. This energy density is not uniform throughout the beam-plasma interaction region, however, because the plasma density varies within the region. This variation of plasma density has two effects: Firstly, the electric field beats with different frequencies at different distances from the axis. When the electric field on the axis is peaking, the field may be going through zero only a millimeter away. Secondly, the electric field is most intense where the plasma frequency is closest to the sixteenth beam harmonic. The elèctron density of the plasma is diffusion controlled so that

$$n_0(r) = (n_0)_{axis} J_0\left(\frac{2.4}{a} r\right) \qquad \text{--- } 19$$

Near the axis,

$$n_0(r) = (n_0)_{axis}\left(1 - \frac{r^2}{4}\right) \qquad \text{--- } 20$$

$$\omega_p^2(r) = (\omega_p^2)_{axis} - \frac{r^2}{4}(\omega_p^2)_{axis} \qquad \text{--- } 21$$

$$\begin{aligned} \varepsilon_r(r) &= (\varepsilon_r)_{axis} + \left(\frac{\omega_p^2}{\omega^2}\right)_{axis}\frac{r^2}{4} \\ &= \left(2\frac{\Delta f}{f}\right)_{axis} + \frac{r^2}{4} \end{aligned} \qquad \text{--- } 22$$

Suppose the plasma frequency on the axis were 20 Mcs greater than the sixteenth harmonic. Then, on the axis, $\varepsilon_r = 2 \times 10^{-3}$. But, according to equation 22, the dielectric constant increases radially. This means that the electric field is most intense near the axis, and the energy density is greatest there. Only 0.27 cm away from the axis the dielectric coefficient increases to 2×10^{-2}, causing the peak energy density to decrease by 1/100.

On the other hand, suppose the plasma frequency on the axis were 20 Mcs smaller than the sixteenth harmonic. Then, on the axis, $\mathcal{E}_r = -2 \times 10^{-3}$. The dielectric coefficient would increase to zero only 0.03 cm away from the axis, in the absence of collisions. The fields cannot actually go to infinity 0.03 cm from the axis because they are limited by a) collisional damping, b) the breakdown of linearity, c) lack of sufficient time for the fields to build up to a high value.

The two cases above are examples of the approach to resonance that can be achieved with the time delay circuit which we have used in our experiment. The latter case is more favorable to the stimulation of plasma electron oscillations, because a small part of the interaction region is much closer to resonance than 20 Mc. There are other conditions possible. For instance, there may be annular parts of the interaction region that are 20 Mc from resonance. The energy stored in the fields during the passage of the beam connot be predicted with great precision because there is no way to assure that any given set of conditions will occur. A calculation of the stored energy is further complicated by the fact that the electric field beats with different beat frequencies at different distances from the axis. This means that when the electric energy density is peaking at one point, it may be going through a minimum at a nearby point.

A typical value of the energy density is the value when $f - f_p$ = 20 Mc, i.e., 3×10^{-2} joules/m^3. The interaction volume is 5×10^{-5} m^3. The total energy stored in the interaction region is expected to be several orders of magnitude above or below

$$3 \times 10^{-2} \text{ joules/m}^3 \times 5 \times 10^{-5} \text{ m}^3 = 10^{-6} \text{ joules.}$$

After the 0.1 μsec burst of electrons has been turned off, most of the stored energy will be dissipated in collisions between oscillating electrons and argon molecules, but some of it is expected to leak out of the vessel. The energy will be dissipated in the time it takes the electrons to make several collisions, a time in the order of 10 μsec. The average rate of dissipation is then 0.1 watts. Only a small fraction of this need leak out to be detected by a sensitive receiver, provided it is not smeared out too thinly over the K-band spectrum.

The electrons oscillating in various parts of the interaction region will do so with different frequencies, because of the non-uniformity of the plasma frequency. According to equation 21, the plasma frequency at the boundary will be about 5% lower (1 kMc) than the plasma frequency on the axis. Furthermore, while the oscillations are damping out, the plasma density continues to decay, changing the plasma frequency at every point in the vessel. Consequently, it is expected that any radiation reaching a receiver outside the vessel will be spread over a broad frequency range.

Suppose that radiation emerged from the vessel at one-millionth of the dissipation ratio. Then the radiated power level might be 10^{-7} watts, based on the estimate above. Suppose that this is uniformly spread over the spectrum with a density of 10^{-7} watts/kMc because of the 1 kMc distribution of plasma frequencies in the interaction region.

The receiver can respond to radiation that is within its two 8 Mcs passbands. (One band is 30 Mc above the intermediate frequency, and the other is 30 Mc below.) So, the level of radiated power that can be detected is 10^{-7} watts x 16 Mc/1000 Mc = 2×10^{-9} watts. Since the antenna can intercept only

1/50 of the radiation emerging from the vessel, the detectable radiation is further reduced to 4×10^{-11} watts, which is somewhat larger than the sensitivity of the receiver 2.5×10^{-11} watts.

So, whether the radiation will be detected depends upon what fraction of the stored energy escapes from the vessel, the rate at which it escapes, and how thinly it is smeared over the spectrum. This experiment was undertaken to determine whether the radiation could be found.

4. Disbursement of Funds

A separate financial report is submitted by the Comptroller.

5. Personnel

Name	Position	Percent Time 1*	2*	3*
E. H. Holt	Professor Senior Investigator	50	75	50
K. C. Stotz	Assistant Professor Assistant Investigator	(50)	100	25
W. C. Taft	Instructor	25	75	terminated Aug 30
R. E. Browne	Research Assistant	100	75	terminated Sept 13
J. S. Mendell	Graduate Assistant	50	100	terminated July 12
R. E. Haskell	Graduate Assistant	(50)	100	terminated Sept 30
D. A. Huchital	Graduate Student	-	(100)	(20)
W. C. Schwartz	Graduate Student	(20)	terminated June 7	
P. N. Y. Pan	Graduate Student	-	-	30
J. Carroll	Undergraduate Student	-	-	20
R. L. Donnerstein	Undergraduate Student	-	-	(15)
L. E. Miller	Undergraduate Student	-	-	(15)
G. M. Mueller	Undergraduate Student	-	-	(15)
J. H. Zablotney	Undergraduate Student	-	-	(15)

Support Personnel

Name	Position	1*	2*	3*
H. Struss	Research Assistant (model shop)	50	25	25
J. Wright	Electronic Technician	50	50	100
R. M. Quinn	Student Technician	25	-	10
C. V. Bhimani	Student Technician	-	100	20
Mrs. M. Santerre	Typist	75	75	25

*1. May 1 - June 7, 1963, Academic year 1962-63.

*2. June 10 - September 13, 1963, Summer 1963.

*3. September 16 - October 31, 1963, Academic year 1963-64.

Note.

Figures in brackets indicate participation in the research without charge to the grant.

6. Program for the Period November 1, 1963 - April 30, 1964

Studies of electromagnetic wave propagation in magnetoplasmas will be made in a guided wave configuration. Measurements of basic plasma processes will be made in a waveguide cell of simplified construction, the original cell being in need of replacement. Work on the positive pulser and the mass spectrometer will continue.

No further work on the electron-beam plasma interaction is planned for this period.

REFERENCES

1. T. H. Stix, Theory of Plasma Waves, McGraw-Hill, 1962.

2. D. A. Huchital, Plasma Research Laboratory, TR 10, p. 26, August, 1963.

3. Ibid, p. 65

4. Ibid, p. 73

5. R. E. Haskell, Plasma Research Laboratory, TR 8, August, 1963.

6. J. E. Rudzki, and E. H. Holt, Plasma Research Laboratory, TR 6, January, 1963.